STATIC AND DYNANIC ANALYSIS OF COMPOSITE PLATE USING THE C^0-TYPE HIGHER-ORDER SHEAR DEFORMATION THEORY

by Tran Vinh Loc[1] - Thai Hoang Chien[1] - Tran Trung Dung[2] - Nguyen Xuan Hung[3]

ABTRACT

This paper presents a novel numerical procedure based on edge-based smoothed finite element method (ES–FEM) in combination with the C^0-type higher-order shear deformation theory (HSDT) for static and dynamic analysis of laminated composite plate. In the present ES–FEM, only the linear approximation is necessary and the discrete shear gap method (DSG) for triangular plate elements is used to avoid the shear locking and spurious zero energy modes. In addition, the stiffness matrices are computed based on smoothing domains associated with the edges of the triangular elements through a strain smoothing technique. Using the C^0-type HSDT, the shear correction factors in the original ES-DSG3 can be removed and replaced by two additional degrees of freedom at each node. Several numerical examples are given to show the performance of the proposed method and results obtained are compared to other available ones.

Keywords: Laminated composite plates, finite element method (FEM), edge-based smoothed finite element method (ES-FEM), C^0-type higher-order shear deformation theory (HSDT).

1. Introduction

Laminated composites are made of two or several laminae layers which are stacked together to obtain desired properties with requirement characteristics such as: higher strength, long fatigue life, corrosion resistance, etc. With the advantageous features they have been used in many practical applications such as aircrafts, aerospace, vehicles, buildings, etc.

Laminated composite plates were widely researched with many various methods. Khdeir and Librescu [1] gave exact solution for static of symmetric cross-ply laminated elastic plates. When the laminated plates becomes thicker, layer- wise (LW) model [2] or 3D elasticity solution [3-5] can be recommended to improve the accuracy of transverse shear stresses. However, 3D has much computational cost. Thus, reduction a 3D problem to a 2D problem based on the equivalent single layer (ESL) theory is considered. Nowadays, ESL theory is developed rapidly with different theories based on various suppositions of displacement field. The simplest theory is classical laminate plate theory (CLPT) – the Kirchoff hypothesis due to ignoring the transverse shear deformation. However, CLPT is inadequate for analysis of thick plates, and hence, the first-order shear deformation theory (FSDT), which considers the effect of shear deformation, is developed. However, in FSDT, strain energy strongly depends on shear correction factor which is based on many factors such as: length to thickness ratio, espect ratio, material, laminated scheme, geometry, boundary condition, etc. In order to overcome the limitations of the FSDT, HSDT was constructed. Reddy *et al.* [6] proposed element for bending, free vibration and stability of laminated plates

[1]*Division of Computational Mechanics, Ton Duc Thang University HCM*
[2]*Faculty of Construction & Electricity, Open University HCM*
[3]*Department of Mechanics, Faculty of Mathematics and Computer Science, University of Science HCM*

according to third order deformation theory (TSDT). The theory that satisfies the free of transverse shear stresses at top and bottom plate's surface needs just 5 degree of freedoms (DOFs) per node like FSDT. But this model requires C^1-continuity of generalized displacements which gets very difficult in calculating derivative. More recently, Shankara and Iyengar [7] developed C^0-continuity element based on Reddy's HSDT with two additional variables have been introduced into the displacement field, and hence only the first derivative of transverse displacement is needed in computing.

In this paper, the ES–DSG approach with some interesting properties such as: (1) super-accurate and super-convergent properties of displacement and stress solutions; (2) be temporally stable and work well for free and forced vibration analyses and (3) be simple to implement without any penalty parameter or additional degrees of freedom [8-14] is further formulated for static analysis of laminated composite plate. In the ES–DSG, the stiffness matrices are obtained basing on the strain smoothing technique over the smoothing domains associated with the edges of the elements. In addition, discrete shear gap technique [15] is used to avoid the shear locking and spurious zero energy modes.

In next section, the formulation is established to analyze laminated composite plate for static and dynamic problem. Some numerical examples are studied to show that present element achieves the high accuracy and agrees well with several other existing elements in the literatures.

2. Problem formulation

2.1. C^0-type higher-order shear deformation theory (HSDT)

Let $\mathrm{u}_0=\{u_0\ v_0\}^T$, w, $\boldsymbol{\beta}=\{\beta_x\ \beta_y\}^T$ and $\boldsymbol{\phi}=\{\phi_x\ \phi_y\}^T$ be the membrane displacements, the transverse displacement of the mid-plane, the rotations in the *y-z* and *x-z* planes and warping function, respectively. The displacements of any point in the plates can be expressed as [7]

$$\begin{aligned} u(x,y,z) &= u_0 + \left(z - \tfrac{4z^3}{3h^2}\right)\beta_x - \tfrac{4z^3}{3h^2}\phi_x \\ v(x,y,z) &= v_0 + \left(z - \tfrac{4z^3}{3h^2}\right)\beta_y - \tfrac{4z^3}{3h^2}\phi_y \quad (-h/2 \le z \le h/2) \\ w(x,y) &= w \end{aligned} \tag{1}$$

In-plane strains through the following equation:

$$\boldsymbol{\varepsilon} = [\varepsilon_{xx}\ \varepsilon_{yy}\ \gamma_{xy}]^T = \boldsymbol{\varepsilon}_0 + z\boldsymbol{\kappa}_1 + z^3\boldsymbol{\kappa}_2 \tag{2}$$

and transverse shear strains are basically defined as

$$\boldsymbol{\gamma} = \begin{bmatrix}\gamma_{xz}\ \gamma_{yz}\end{bmatrix}^T = \boldsymbol{\varepsilon}_s + z^2\boldsymbol{\kappa}_s \tag{3}$$

where

$$\boldsymbol{\varepsilon}_0 = \nabla_s \mathbf{u}_0 \qquad \boldsymbol{\kappa}_1 = \frac{1}{2}\left\{\nabla\boldsymbol{\beta} + (\nabla\boldsymbol{\beta})^T\right\} \qquad \boldsymbol{\kappa}_2 = \frac{c}{6}\left\{\left(\nabla\boldsymbol{\phi} + (\nabla\boldsymbol{\phi})^T\right) + \left(\nabla\boldsymbol{\beta} + (\nabla\boldsymbol{\beta})^T\right)\right\}$$

$$\boldsymbol{\varepsilon}_s = \nabla w + \boldsymbol{\beta} \qquad \boldsymbol{\kappa}_s = c\left(\boldsymbol{\beta} + \boldsymbol{\phi}\right) \qquad \text{with } c = -4/h^2 \tag{4}$$

From Hook's law the stress in plane is (see more [7])

$$[\boldsymbol{\sigma}\quad \boldsymbol{\tau}]^T = \overline{\mathbf{Q}}[\boldsymbol{\varepsilon}\quad \boldsymbol{\gamma}]^T \tag{5}$$

A weak form of the static model for laminated composite plates can be briefly expressed as:

$$\int_\Omega \delta\boldsymbol{\varepsilon}_p^T \mathbf{D}^* \boldsymbol{\varepsilon}_p d\Omega + \int_\Omega \delta\boldsymbol{\gamma}^T \mathbf{D}_S^* \boldsymbol{\gamma} d\Omega = \int_\Omega \delta w p d\Omega \tag{6}$$

where p is the transverse loading per unit area and

$$\mathbf{D}^* = \begin{bmatrix} \mathbf{A} & \mathbf{B} & \mathbf{E} \\ \mathbf{B} & \mathbf{D} & \mathbf{F} \\ \mathbf{E} & \mathbf{F} & \mathbf{H} \end{bmatrix},\ \boldsymbol{\varepsilon}_p = \begin{bmatrix} \boldsymbol{\varepsilon}_0 \\ \boldsymbol{\kappa}_1 \\ \boldsymbol{\kappa}_2 \end{bmatrix} \tag{7}$$

$$\left(A_{ij}, B_{ij}, D_{ij}, E_{ij}, F_{ij}, H_{ij}\right) = \int_{-h/2}^{h/2} \left(1, z, z^2, z^3, z^4, z^6\right) Q_{ij} dz \quad i, j = 1, 2, 6$$

$$\mathbf{D}_S^* = \begin{bmatrix} \mathbf{A}^S & \mathbf{B}^S \\ \mathbf{B}^S & \mathbf{D}^S \end{bmatrix},\ \boldsymbol{\gamma} = \begin{bmatrix} \boldsymbol{\varepsilon}_s \\ \boldsymbol{\kappa}_s \end{bmatrix} \tag{8}$$

$$\left(A_{ij}^s, B_{ij}^s, D_{ij}^s\right) = \int_{-h/2}^{h/2} \left(1, z^2, z^4\right) Q_{ij} dz \quad i, j = 4, 5$$

For the free vibration analysis, a weak form of composite plates can be derived from the following dynamic equation

$$\int_\Omega \delta\boldsymbol{\varepsilon}_p^T \mathbf{D}^* \boldsymbol{\varepsilon}_p d\Omega + \int_\Omega \delta\boldsymbol{\gamma}^T \mathbf{D}_S^* \boldsymbol{\gamma} d\Omega = \int_\Omega \delta \mathbf{u}^T \mathbf{m} \ddot{\mathbf{u}} d\Omega \tag{9}$$

where **m** is defined as :

$$\mathbf{m} = \begin{bmatrix} I_1 & 0 & 0 & I_2 & 0 & c/3I_4 & 0 \\ & I_1 & 0 & 0 & I_2 & 0 & c/3I_4 \\ & & I_1 & 0 & 0 & 0 & 0 \\ & & & I_3 & 0 & c/3I_5 & 0 \\ & & & & I_3 & 0 & c/3I_5 \\ & & & & & c^2/9I_7 & 0 \\ sym & & & & & & c^2/9I_7 \end{bmatrix} \tag{10}$$

with $$\left(I_1, I_2, I_3, I_4, I_5, I_7\right) = \int_{-t/2}^{t/2} \rho\left(1, z, z^2, z^3, z^4, z^6\right) dz$$

2.2. The formulation of three-node triangular element with stabilized discrete shear gap technique (DSG3)

The geometry domain Ω is discretized into N_e triangular elements with N_e number of nodes. The displacement field **u** in the element domain can be approximate as

$$\mathbf{u}^h(x) = \sum_{I=1}^{n} \mathbf{N}_I(x) \mathbf{d}_I \tag{11}$$

where n is total number of nodes located in the element domain, **N** is the shape function and the nodal degrees of freedom associated to node I is $\mathbf{d}_I = \left[u_0\ v_0\ w\ \beta_x\ \beta_y\ \phi_x\ \phi_y\right]^T$

The strains in Eq.(7) and (8) can be expressed to following nodal displacements as:

$$\left[\boldsymbol{\varepsilon}_p \quad \boldsymbol{\gamma}\right]^T = \sum_{I=1}^{n} \left[\mathbf{B}_I^m \ \mathbf{B}_I^{b1} \ \mathbf{B}_I^{b2} \ \mathbf{B}_I^{s0} \ \mathbf{B}_I^{s1}\right]^T \mathbf{d}_I \tag{12}$$

where B_I are generalized strain-displacement matrices gained from derivative of shape function.

$$\mathbf{B}_I^m = \begin{bmatrix} N_{i,x} & 0 & 0 & 0 & 0 & 0 & 0 \\ 0 & N_{i,y} & 0 & 0 & 0 & 0 & 0 \\ N_{i,y} & N_{i,x} & 0 & 0 & 0 & 0 & 0 \end{bmatrix}, \mathbf{B}_I^{b1} = \begin{bmatrix} 0 & 0 & 0 & N_{i,x} & 0 & 0 & 0 \\ 0 & 0 & 0 & 0 & N_{i,y} & 0 & 0 \\ 0 & 0 & 0 & N_{i,y} & N_{i,x} & 0 & 0 \end{bmatrix}$$

$$\mathbf{B}_I^{s0} = \begin{bmatrix} 0 & 0 & N_{i,x} & N_i & 0 & 0 & 0 \\ 0 & 0 & N_{i,y} & 0 & N_i & 0 & 0 \end{bmatrix}, \mathbf{B}_I^{s1} = c\begin{bmatrix} 0 & 0 & 0 & N_i & 0 & N_i & 0 \\ 0 & 0 & 0 & 0 & N_i & 0 & N_i \end{bmatrix} \quad (13)$$

$$\mathbf{B}_I^{b2} = \frac{c}{3}\begin{bmatrix} 0 & 0 & 0 & N_{i,x} & 0 & N_{i,x} & 0 \\ 0 & 0 & 0 & 0 & N_{i,y} & 0 & N_{i,y} \\ 0 & 0 & 0 & N_{i,y} & N_{i,x} & N_{i,y} & N_{i,x} \end{bmatrix}$$

It is well known that with the lower-order degree elements shear locking often occurs in the limit of thin plates. To overcome this drawback, we based on the Discrete-Shear-Gap (DSG) technique to approximate the shear strain field. (cf. Bletzinger *et al.* [15] for more detail)

$$\varepsilon_s = (\Delta\varepsilon_s)' = \sum_{i=1}^{n} \frac{dN^i}{dx}\Delta\varepsilon_s^i \quad (14)$$

In DSG3 technique, $\mathbf{B}_I^{s0}$ is directly derived from the nodal coordinates.

$$\mathbf{B}_{DSG}^{s0} = \frac{1}{\det J}\left[\begin{array}{ccccccc|ccccccc|ccccccc} 0 & 0 & b-c & \frac{\det J}{2} & 0 & 0 & 0 & 0 & 0 & c & \frac{ac}{2} & \frac{bc}{2} & 0 & 0 & 0 & 0 & -b & -\frac{bd}{2} & -\frac{bc}{2} & 0 & 0 \\ 0 & 0 & d-a & 0 & \frac{\det J}{2} & 0 & 0 & 0 & 0 & -d & -\frac{ad}{2} & -\frac{bd}{2} & 0 & 0 & 0 & 0 & a & \frac{ad}{2} & \frac{ac}{2} & 0 & 0 \end{array}\right]$$

with $a = x_2 - x_1, b = y_2 - y_1, c = y_3 - y_1, d = x_3 - x_1$ and det $J=ac - bd$ where x_i, y_i i=1,2,3 are the coordinates of node.

2.3. A formulation of ES-FEM

In the ES-FEM, the strains are "smoothed" over local smoothing domains, and naturally the computation for the stiffness matrix is no longer based on elements, but on these smoothing domains. These smoothing domains are constructed based on the edges of the elements such that $\Omega \approx \bigcup_{k=1}^{N_{ed}} \Omega^{(k)}$ and $\Omega^{(i)} \cap \Omega^{(j)} = \varnothing$ for $i \neq j$, in which N_{ed} is the total number of edges of all elements in the entire problem domain. For triangular elements, the smoothing domain $\Omega^{(k)}$ associated with the edge k is created by connecting two end-nodes of the edge to centroids of adjacent elements as depicted in Figure 1.

Figure 1: Division of domain into triangular element and smoothing cells $\Omega^{(k)}$ connected to edge k of triangular elements.

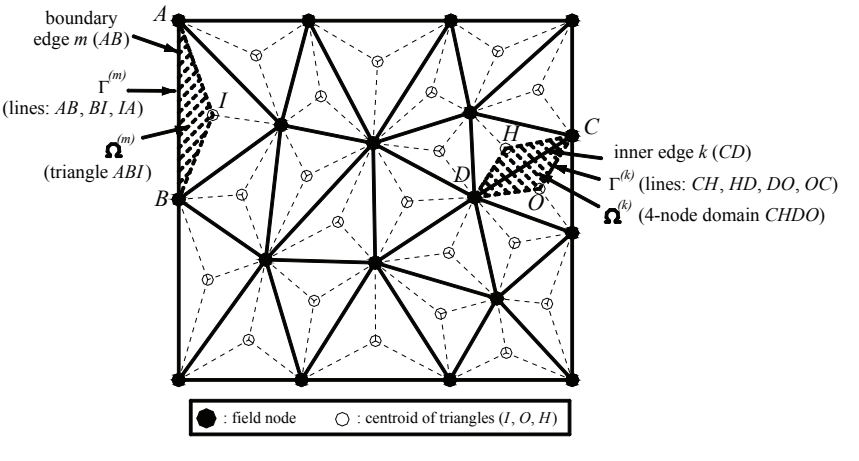

Introducing smoothing membrane, curvature and shear strains over the smoothing domain $\Omega^{(k)}$, we have

$$\tilde{\varepsilon}_k = \int_{\Omega^{(k)}} \varepsilon^h(\mathbf{x})\Phi(\mathbf{x})d\Omega \tag{16}$$

where smoothing function $\Phi(x)$ is assumed to be a piecewise constant function and is given by

$$\Phi(\mathbf{x}) = \begin{cases} 1/A^{(k)} & \mathbf{x} \in \Omega^{(k)} \\ 0 & \mathbf{x} \notin \Omega^{(k)} \end{cases} \tag{17}$$

Substitute Eq.(17) into Eq.(16), the smoothed strains of the ES-DSG3 become

$$\tilde{\varepsilon}_k = \frac{1}{A^{(k)}} \int_{\Omega^{(k)}} \varepsilon^h d\Omega \tag{18}$$

where $A^{(k)}$ is the area of the smoothing cell $\Omega^{(k)}$ and is computed by

$$A^{(k)} = \int_{\Omega^{(k)}} d\Omega = \frac{1}{3}\sum_{i=1}^{N_e^k} A_i \tag{19}$$

where N_e^k is the number of elements containing the edge k (N_e^k=1 for the boundary edges and N_e^k=2 for inner edges as shown in Figure 1 and A_i is the area of the i^{th} element around the edge k.

Then smoothed strain matrix is expressed as

$$\tilde{\mathbf{B}}_I(\mathbf{x}_k) = \frac{1}{A^{(k)}} \int_{\Omega^{(k)}} \mathbf{B}_I(\mathbf{x}) \mathrm{d}\Omega \tag{20}$$

In the triangular DSG3 element, a shape function is linear. Hence, Eq. (20) can be reformulated for the constant strain matrices

$$\begin{aligned} &\tilde{\mathbf{B}}_I^m(\mathbf{x}_k) = \frac{1}{A^{(k)}}\sum_{i=1}^{N_e^k} A_i \mathbf{B}_i^m,\ \tilde{\mathbf{B}}_I^{b1}(\mathbf{x}_k) = \frac{1}{A^{(k)}}\sum_{i=1}^{N_e^k} A_i \mathbf{B}_i^{b1} \\ &\tilde{\mathbf{B}}_I^{b2}(\mathbf{x}_k) = \frac{1}{A^{(k)}}\sum_{i=1}^{N_e^k} A_i \mathbf{B}_i^{b2},\ \tilde{\mathbf{B}}_I^{s0}(\mathbf{x}_k) = \frac{1}{A^{(k)}}\sum_{i=1}^{N_e^k} A_i \mathbf{B}_{i-DSG}^{s0} \end{aligned} \tag{21}$$

Only the linear strain matrix $\mathbf{B}_I^{s1}$ needs to be refined

$$\tilde{\mathbf{B}}_I^{s1}(\mathbf{x}_k) = \frac{1}{A^{(k)}}\sum_{i=1}^{N_e^k} \int_{A_i} \mathbf{B}_I^{s1}(\mathbf{x})\mathrm{d}\Omega = \frac{c}{9A^{(k)}}\sum_{i=1}^{N_e^k} A_i \mathbf{B}^* \tag{22}$$

where

$$\mathbf{B}^* = \begin{bmatrix} 0 & 0 & 0 & 1 & 0 & 1 & 0 \\ 0 & 0 & 0 & 0 & 1 & 0 & 1 \end{bmatrix} \tag{23}$$

Therefore, the global stiffness matrix of the ES-DSG3 element is assembled by

$$\tilde{\mathbf{K}} = \sum_{k=1}^{N_n} \tilde{\mathbf{K}}^{(k)} \tag{24}$$

in which the edge-based stiffness matrix is computed as follows

$$\begin{aligned} \tilde{\mathbf{K}}^{(k)} = &\left[\left(\tilde{\mathbf{B}}_I^m\right)^T \mathbf{A}\tilde{\mathbf{B}}_I^m + \left(\tilde{\mathbf{B}}_I^m\right)^T \mathbf{B}\tilde{\mathbf{B}}_I^{b1} + \left(\tilde{\mathbf{B}}_I^m\right)^T \mathbf{E}\tilde{\mathbf{B}}_I^{b2}\right] A^{(k)} \\ &+\left[\left(\tilde{\mathbf{B}}_I^{b1}\right)^T \mathbf{B}\tilde{\mathbf{B}}_I^m + \left(\tilde{\mathbf{B}}_I^{b1}\right)^T \mathbf{D}\tilde{\mathbf{B}}_I^{b1} + \left(\tilde{\mathbf{B}}_I^{b1}\right)^T \mathbf{F}\tilde{\mathbf{B}}_I^{b2}\right] A^{(k)} \\ &+\left[\left(\tilde{\mathbf{B}}_I^{b2}\right)^T \mathbf{E}\tilde{\mathbf{B}}_I^m + \left(\tilde{\mathbf{B}}_I^{b2}\right)^T \mathbf{F}\tilde{\mathbf{B}}_I^{b1} + \left(\tilde{\mathbf{B}}_I^{b2}\right)^T \mathbf{H}\tilde{\mathbf{B}}_I^{b2}\right] A^{(k)} \\ &+\left[\left(\tilde{\mathbf{B}}_{I-DSG}^{s0}\right)^T \mathbf{A}^S\tilde{\mathbf{B}}_{I-DSG}^{s0} + \left(\tilde{\mathbf{B}}_{I-DSG}^{s0}\right)^T \mathbf{B}^S\tilde{\mathbf{B}}_I^{s1} + \left(\tilde{\mathbf{B}}_I^{s1}\right)^T \mathbf{B}^S\tilde{\mathbf{B}}_{I-DSG}^{s0} + \left(\tilde{\mathbf{B}}_I^{s1}\right)^T \mathbf{D}^S\tilde{\mathbf{B}}_I^{s1}\right] A^{(k)} \end{aligned} \tag{25}$$

To solve Eq.(6), the solution of static equilibrium equation is expressed

$$\tilde{\mathbf{K}}\mathbf{d} = \mathbf{F} \tag{26}$$

where the load vector

$$\mathbf{F} = \int_{\Omega} p\mathbf{N}\mathrm{d}\Omega \tag{27}$$

For free vibration problem, we solve Eq. (9) to find natural frequency $\omega \in \mathrm{R}^{+}$ such that

$$\left(\tilde{\mathbf{K}} - \omega^2\mathbf{M}\right)\mathbf{d} = \mathbf{0} \tag{28}$$

where $\mathbf{M}$ is the global mass matrix given by

$$\mathbf{M} = \int_{\Omega} \mathbf{N}^T\mathbf{m}\mathbf{N}\mathrm{d}\Omega \tag{29}$$

3. Nummerical results

3.1. Convergence study

First, let's consider the model of an isotropic square plate with simply supported condition and length-to-thickness ratio $a/h = 10$. The plate having the Young's modulus E and the Poisson's ratio v=0.25 subjected to uniform load.

The central displacement and axial stress are normalized as $\bar{w} = 10^2 wEh^3/(q_0a^4)$ $\bar{\sigma} = \sigma h^2/(q_0a^2)$, respectively. Figure 2 plotted the comparision between present result with several other methods such as: DSG3, MITC4, MRBF [19] and the exact solution [18]. It can be seen that ES-DSG3 solutions are closed to those of MITC4. The results are in good agreement with solutions by Akhras [18]. With uniform mesh 16x16x2, the error between them is 0.84% for deflection and 0.40% for axial stress, respectively.

Figure 2. Simply supported isotropic square plate (*a/h*=10)

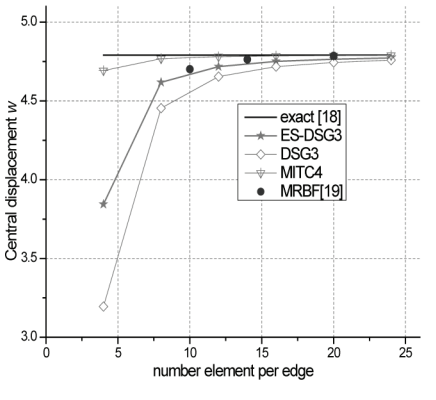

(a) Central displacement

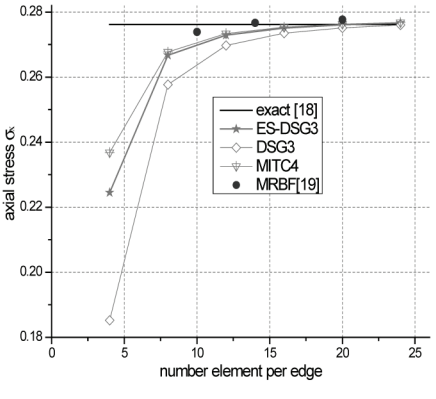

(b) Axial stress

3.2. Composite square plate

a) Static analysis

In this section, material properties of plate are assumed $E_1 = 25E_2$; $G_{12} = G_{13} = 0.5E_2$; $G_{23} = 0.2E_2$; $v_{12} = 0.25$. The simply supported square [0/90/90/0] laminated plate subjected to sinusoidal load $P_z = P\sin\left(\frac{\pi x}{a}\right)\sin\left(\frac{\pi y}{b}\right)$. The normalized displacement $\bar{w} = 100wEh^3/(qa^4)$, normal inplane stresses $\bar{\sigma} = \sigma h^2/\left(qa^2\right)$ and normal transverse shear stresses $\bar{\tau} = \tau h^2/\left(qa\right)$ are presented in Table 1. Some comments are given here: (1) the present results agree well with those of [3, 2, 6,16 18, 19, 21], especially for thick plates and compared with the solution of 3D elasticity results [3], the solution of the ES-DSG3 is slightly nearer than those of Reddy [6], Ferreira [1919], and finite strip method [18]; (2) HSDT models give higher transverse

deflection and in-plane streses than FSDT models and the difference between them is lessened according to decrement of plate's thickness; (3) however, the opposite results are obtained for shear stress $\bar{\tau}_{xz}$. Figure 3 plots the distribution of stresses through thickness plate with *a/h*=4, 10 respectively. It can be seen that the shear stresses are free on the bounding planes and distribute parabolically through thickness of laminae. They are as same as that given in Reddy's theory[16]

Table 1: simply supported [0/90/90/0] square laminated plate under sinusoidal load

a/h	method	*w*	$\bar{\sigma}_x(\frac{a}{2},\frac{b}{2},\frac{h}{2})$	$\bar{\sigma}_y(\frac{a}{2},\frac{b}{2},\frac{h}{4})$	$\bar{\sigma}_{xy}(0,0,\frac{h}{2})$	$\bar{\sigma}_{yz}(\frac{a}{2},0,0)$	$\bar{\sigma}_{xz}(0,\frac{b}{2},0)$
	Strip HSDT [18]	1.8939	0.6806	0.6463	0.045		0.2109
	RBF-PS [21]	1.9023	0.7057	0.6309	0.0461		0.2138
	MRBF HSDT [19]	1.8864	0.6659	0.6313	0.0433		0.1352
	Layerwise [2]	1.9075	0.6432	0.6228	0.0441		0.2166
4	3D Elasticity [3]	1.9540	0.7200	0.6660	0.0467		0.2700
	TSDT (Reddy) [6]	1.8937	0.6651	0.6322	0.044	0.239	0.2064
	ES-DSG3	**1.9046**	**0.7005**	**0.6236**	**0.0476**	**0.2387**	**0.2071**
	FSDT (Reddy) [6]	1.710	0.4059	0.5765	0.0308	0.196	0.1398
	HCM [21]	1.7095	0.4059	0.5764	0.0308		0.2686
	Strip HSDT [18]	0.7149	0.5589	0.3974	0.0273		0.2697
	RBF-PS [21]	0.7204	0.5609	0.3911	0.0273		0.2843
	MRBF HSDT [19]	0.7153	0.5466	0.4383	0.0267		0.3347
	Layerwise [2]	0.7309	0.5496	0.3956	0.0273		0.2888
10	3D Elasticity [3]	0.743	0.559	0.403	0.0276		0.301
	TSDT (Reddy) [6]	0.7147	0.5456	0.3888	0.0268	0.1530	0.2640
	ES-DSG3	**0.7179**	**0.5554**	**0.3867**	**0.0288**	**0.1560**	**0.2793**
	FSDT (Reddy) [6]	0.6628	0.4989	0.3615	0.0241	0.130	0.1667
	HCM [21]	0.6627	0.4989	0.3614	0.0241		0.3181
	Strip HSDT [18]	0.4343	0.5507	0.2769	0.0217		0.2948
	RBF-PS [2121]	0.432	0.5387	0.2697	0.0213		0.3154
	MRBF HSDT [19]	0.4365	0.5413	0.3359	0.0215		0.4106
	Layerwise [2]	0.4374	0.542	0.2697	0.0216		0.3232
100	3D Elasticity [3]	0.4347	0.539	0.271	0.0214		0.339
	TSDT (Reddy) [6]	0.4343	0.5387	0.2708	0.0213	0.139	0.2897
	ES-DSG3	**0.4310**	**0.5331**	**0.2680**	**0.0213**	**0.1365**	**0.3222**
	FSDT (Reddy) [6]	0.4337	0.5382	0.2705	0.0213	0.139	0.178
	HCM [21]	0.4337	0.5382	0.2704	0.0213		0.339

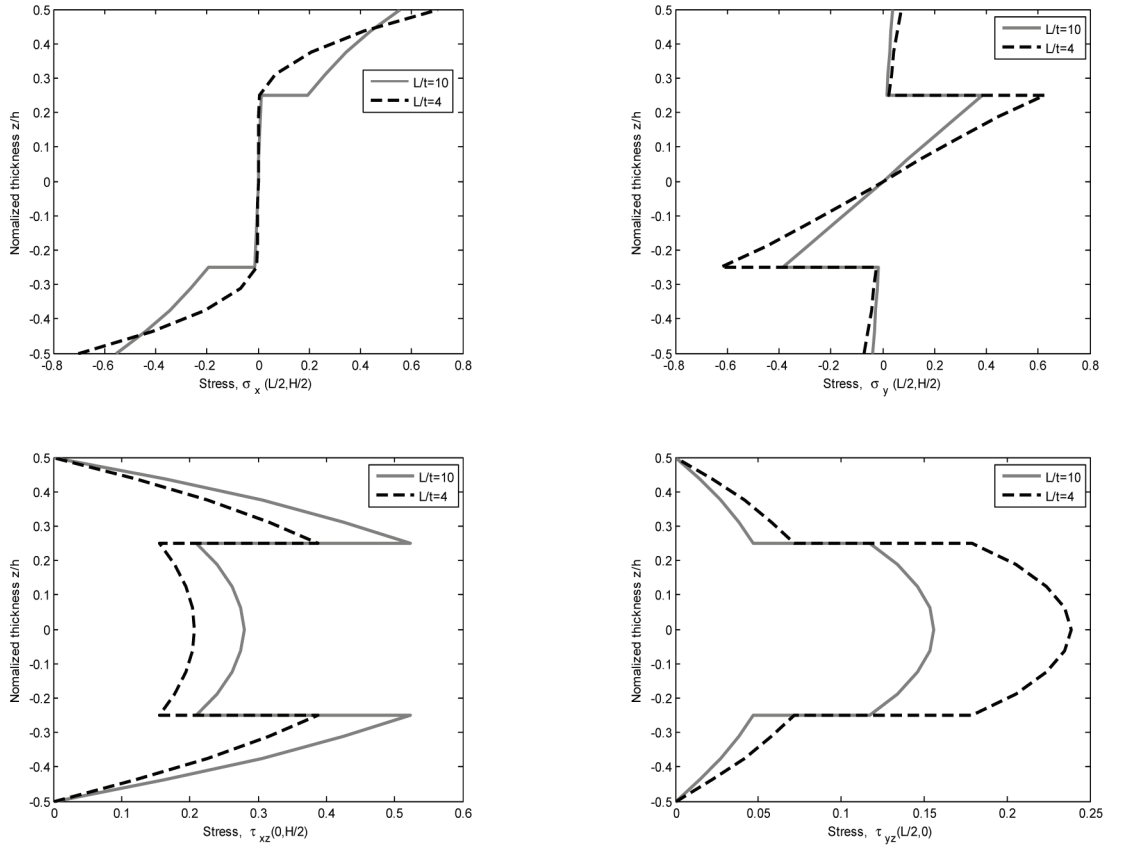

b) Dynamic analysis

Let's consider a [0/90/0] laminated square plate with clamped boundary and the material properties which are assumed as $E_1 = 40E_2$; $G_{12} = G_{13} = 0.6E_2$; $G_{23} = 0.5E_2$; $\nu_{12} = 0.25$; $\rho = 1$. This problem has been previously investigated by a number of authors. For example, it was reported by Liew [22] using the p-Ritz method; Zen and Wanji [24] based on global-local higher-order theory (GLHOT); Ferreira and Fasshauer [23] applied RBF-Pseudospectral method based on FSDT and SongXiang *et al.* [25] with n^{th}-order shear deformation theory (nOSDT). The first six frequency $\bar{\omega} = \omega b^2 / \pi^2 \sqrt{\rho h / D_0}$ with $D_0 = E_2 h^3 / \left[12\left(1-\nu_{12}\nu_{21}\right)\right]$ are listed in Table 2 corresponding several different values of length-to-thickness ratio *a/h*. It is obvious that, results of ES-DSG3 are closer to solutions of [23] than those of MITC4 and DSG3. However, for thin plates (*a/h* ≥100) the error of frequencies between present element and the element in [23] is larger because of predominant transverse shear effect. The first six mode shapes of plate with *a/h* =10 are plotted in Figure 4.

Table 2: Effect of *a/h* ratio on frequency parameters for clamped [0/90/0] laminated plate

a/h	method	1	2	3	4	5	6
5	**ES-DSG3**	**4.5179**	**6.5328**	**8.0316**	**9.3844**	**9.5085**	**11.7461**
	MITC4	4.5290	6.5691	8.0944	9.4127	9.6190	11.7727
	DSG3	4.5534	6.6407	8.1327	9.5640	9.7983	12.1304
	p-Ritz [22]	4.447	6.642	7.700	9.185	9.738	11.399
	GLHOT[24]	4.450	6.524	8.178	9.473	9.492	11.769
	nOSDT[25]	4.5299	6.7573	7.9514	9.4432	9.9118	11.9357
	RBF-PS[23]	4.5141	6.508	8.0361	9.3468	9.3929	11.5749
10	**ES-DSG3**	**7.4938**	**10.3571**	**14.2525**	**15.1791**	**16.1445**	**19.7699**
	MITC4	7.5140	10.4044	14.4102	15.4531	16.1828	19.8828
	DSG3	7.5675	10.5724	14.4863	15.6636	16.6419	20.5875
	p-Ritz [22]	7.411	10.393	13.913	15.429	15.806	19.572
	GLHOT[24]	7.484	10.207	14.340	14.863	16.070	19.508
	nOSDT[25]	7.5237	10.5178	14.2499	15.6112	16.1393	19.9320
	RBF-PS[23]	7.4727	10.2544	14.244	14.9363	15.9807	19.4129
20	**ES-DSG3**	**11.0510**	**14.2606**	**20.8535**	**23.5526**	**25.6538**	**29.9509**
	MITC4	11.0643	14.2039	20.9486	23.8088	25.5792	30.0418
	DSG3	11.1696	14.5723	21.5668	23.9760	26.4457	31.1711
	p-Ritz [22]	10.953	14.028	20.388	23.196	24.978	29.237
	GLHOT[24]	11.003	14.064	20.321	23.498	25.350	29.118
	nOSDT[25]	11.0583	14.1351	20.5235	23.5759	25.3572	29.5575
	RBF-PS[23]	10.968	13.9636	20.0983	23.3572	25.0859	28.6749
100	**ES-DSG**	**14.6428**	**18.0439**	**25.9557**	**38.8029**	**39.0436**	**41.5313**
	MITC4	14.6029	17.7088	25.3614	38.3778	38.9773	40.6314
	DSG3	14.9188	18.9300	27.9059	39.8095	42.4919	43.7475
	p-Ritz [22]	14.666	17.614	24.511	35.532	39.157	40.768
	GLHOT[24]	14.601	17.812	25.236	37.168	38.528	40.668
	RBF-PS[23]	14.4305	17.3776	24.2662	35.5596	37.7629	39.3756

Figure 4. The first six mode shapes of a clamped [0/90/0] laminated plate with ratio *a/h* = 10.

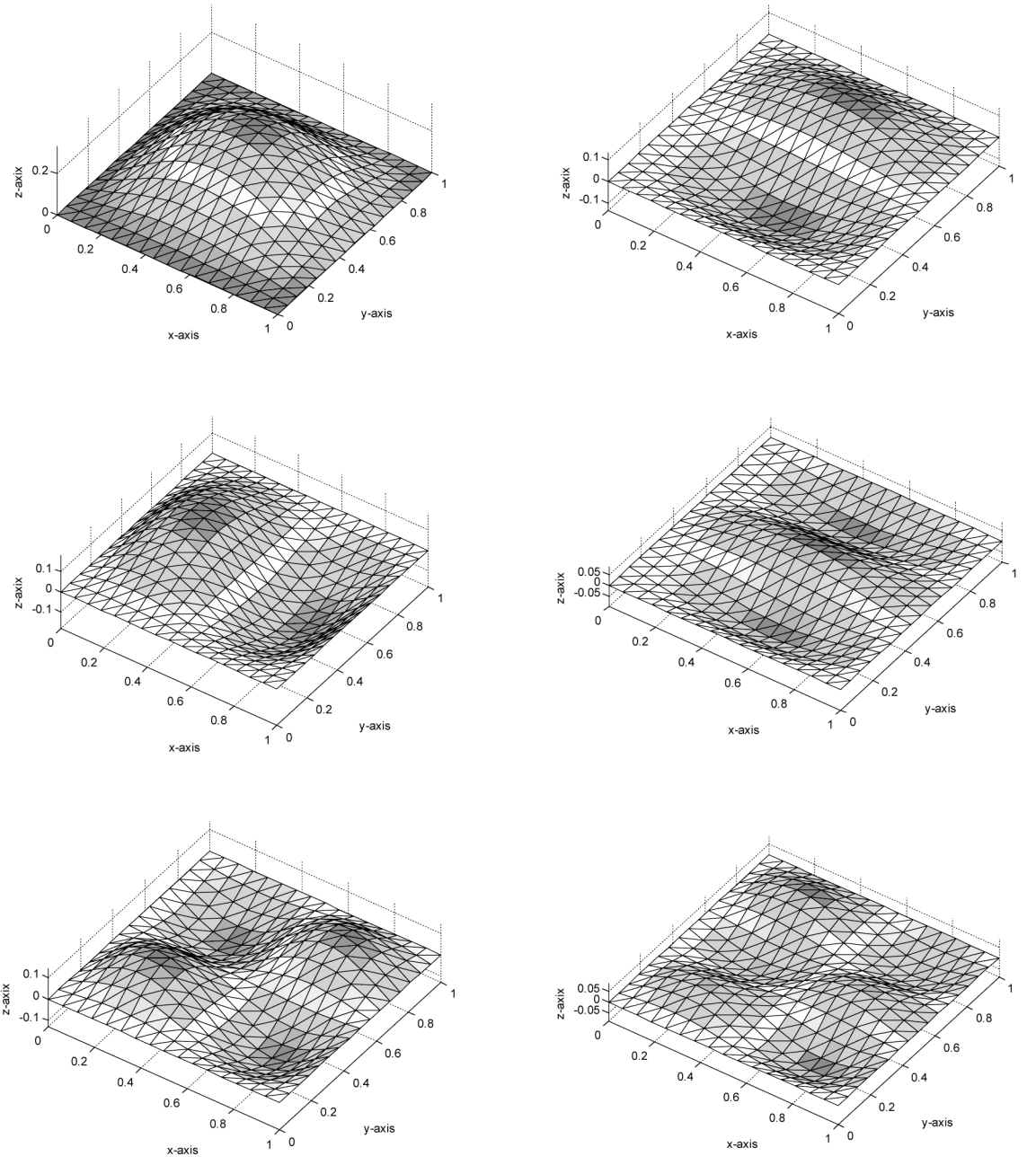

4. Conclusions

The paper presents the combination of the ES-DSG3 and the C^0-type higher-order shear deformation theory (HSDT) to give a new linear triangular plate element for static and dynamic analysis of laminated composite plates. In this element, the stiffness matrices are simply obtained based on the strain smoothing technique over smoothing domains associated with the edges of triangular elements. Using the C^0-type HSDT, the shear correction factors in the original ES-DSG3 can be removed and replaced by two additional degrees of freedom at each node. The results of the ES-DSG3 element also agree well with analytical solution and show remarkably excellent performance compared to results of several other published elements in the literature.

REFERENCES

1. A.A. Khdeir, L. Librescu. Analysis of symmetric cross-ply laminated elastic plates using a higher-order theory: part I stress and displacement. Compos Struct **9** (1988) 189-213.

2. A.J.M. Ferreira. Analysis of composite plates using a layerwise deformation theory and multiquadrics discretization. Mech Adv Mater Struct **12** (2005) 99–112.

3. N.J. Pagano. Exact solutions for rectangular bidirectional composites and sandwich plates. J Compos Mater **4** (1970) 20–34.

4. A.K. Noor. Free vibration of multilayered composite plates. AIAA.J 11 (1973) 1038–9.

5. A.K. Noor. Stability of multilayered composite plates. Fiber Sci Tech 8 (1975) 81-9.

6. J.N. Reddy. A simple higher-order theory for laminated composite plates. J Appl Mech **51** (1984) 745–52.

7. Shankara CA, Iyengar NGR. A C^0 element for the free vibration analysis of laminated composite plates. Journal of Sound and Vibration **191** (1996) 721-738.

8. Nguyen-Xuan H, Liu GR, Thai-Hoang C, Nguyen-Thoi T. An edge-based smoothed finite element method with stabilized discrete shear gap technique for analysis of Reissner-Mindlin plates. Comput Methods Appl Mech Eng **199** (2010) 471–89.

9. Liu GR, Dai KY, Nguyen TT. A smoothed finite element for mechanics problems. Comput Mech **39** (2007) 859–77.

10. Nguyen-Thanh N, Rabczuk T, Nguyen-Xuan H, Bordas S. A smoothed finite element method for plate analysis. Comput Methods Appl Mech Eng **198** (2008)165–77.

11. Nguyen-Xuan H, Liu GR, Nguyen-Thoi T, Nguyen Tran C. An edge – based smoothed finite element method (ES-FEM) for analysis of two–dimensional piezoelectric structures. Smart Materials Struct **18** (2009) 065015.

12. Nguyen-Thoi T, Liu GR, Vu-Do HC, Nguyen-Xuan H. *An edge –based smoothed finite element method (ES-FEM) for visco-elastoplastic analyses of 2D solids using triangular mesh.* Comput Mech **45** (2009) 23-44.

13. **H. Nguyen-Xuan**, Loc V. Tran, T. Nguyen-Thoi, H.C Vu Do, *Analysis of functionally graded plates using an edge-based smoothed finite element method*, Composite Structures, in press, doi:10.1016/j.compstruct.2011.04.028, 2011.

14. Chen JS, Wu CT, Yoon S, You Y. A stabilized conforming nodal integration for Galerkin mesh-free methods. Int J Numer Methods Eng **50** (2001) 435–66.

15. Bletzinger KU, Bischoff M, Ramm E. A unified approach for shear-locking free triangular and rectangular shell finite elements. Comput Struct **75** (2000) 321–34.

16. J.N. Reddy. Mechanics of laminated composite plates-theory and analysis. NewYork: CRC Press;1997.

17 Bathe KJ, Dvorkin EN. A four-node plate bending element based on Mindlin/ Reissener plate theory and a mixed interpolation. Int J Numer Methods Eng **21** (1985) 367–83.

18. G. Akhras, M.S. Cheung, W. Li. Finite strip analysis for anisotropic laminated composite plates using higher-order deformation theory. Comput Struct **52** (1994) 471–7

19. A.J.M. Ferreira, C.M.C. Roque, P.A.L.S. Martins. Analysis of composite plates using higher-order shear deformation theory and a finite point formulation based on the multiquadric radial basis function method. Compos: Part B **34** (2003) 627–36.
20. J.N. Reddy. Introduction to the finite element method. NewYork:McGraw-Hill;1993.
21. A.J.M. Ferreira, Luís M.S. Castro, Silvia Bertoluzza. A high order collocation method for the static and vibration analysis of composite plates using a first-order theory. Composite Structures **34** (2003) 627-636.
22. K.M. Liew. Solving the vibration of thick symmetric laminates by Reissner/Mindlin plate theory and the p-Ritz method. J. Sound Vib.**198** (1996) 343–60.
23. A.J.M. Ferreira and G.E. Fasshauer. Natural frequencies of shear deformable beams and plates by a RBF-Pseudospectral method. Comput. Methods Appl. Mech. Eng.**196** (2006) 134–46.
24. W. Zhen, C. Wanji. Free vibration of laminated composite and sandwich plates using global-local higher-order theory. J. Sound Vib. **298** (2006) 333–49.
25. Song Xiang, Shao-xi Jiang, Ze-yang Bi, Yao-xing Jin, Ming-sui Yang. A nth-order meshless generalization of Reddy's third-order shear deformation theory for the free vibration on laminated composite plates. Compos. Struct.**93** (2011) 299–307.